



**HAL**  
open science

# Gas phase growth of metal-organic frameworks on microcantilevers for highly sensitive detection of volatile organic compounds

Masoud Akbari, Hamza Mouharrar, Chiara Crivello, Martial Defoort, Eihab Abdel-Rahman, Skandar Basrour, Kevin Musselman, David Munoz-Rojas

## ► To cite this version:

Masoud Akbari, Hamza Mouharrar, Chiara Crivello, Martial Defoort, Eihab Abdel-Rahman, et al.. Gas phase growth of metal-organic frameworks on microcantilevers for highly sensitive detection of volatile organic compounds. *APL Materials*, 2024, 12 (6), pp.1119. 10.1063/5.0206295 . hal-04626045

**HAL Id: hal-04626045**

<https://hal.science/hal-04626045v1>

Submitted on 23 Oct 2024

**HAL** is a multi-disciplinary open access archive for the deposit and dissemination of scientific research documents, whether they are published or not. The documents may come from teaching and research institutions in France or abroad, or from public or private research centers.

L'archive ouverte pluridisciplinaire **HAL**, est destinée au dépôt et à la diffusion de documents scientifiques de niveau recherche, publiés ou non, émanant des établissements d'enseignement et de recherche français ou étrangers, des laboratoires publics ou privés.



Distributed under a Creative Commons Attribution - NonCommercial 4.0 International License

# Gas Phase Growth of Metal-Organic Frameworks on Microcantilevers for Highly Sensitive Detection of Volatile Organic Compounds

Masoud Akbari<sup>1,2,3</sup>, Hamza Mouharrar<sup>4</sup>, Chiara Crivello<sup>5</sup>, Martial Defoort<sup>2</sup>, Eihab Abdel-Rahman<sup>4</sup>, Skandar Basrour<sup>2,\*</sup>, Kevin Musselman<sup>3,\*</sup>, David Muñoz-Rojas<sup>1,\*</sup>

1. Univ. Grenoble Alpes, CNRS, Grenoble INP, LMGP, 38000 Grenoble, France
2. Univ. Grenoble Alpes, CNRS, Grenoble INP, TIMA, 38000 Grenoble, France
3. Department of Mechanical and Mechatronics Engineering, University of Waterloo, Waterloo, Canada
4. Department of Systems Design Engineering, University of Waterloo, Waterloo, Canada
5. IEMN, UMR CNRS 8520, Av Poincaré - CS60069, 59652 Villeneuve d'Ascq Cedex, France

## Abstract

A gas-phase technique, known as chemical vapor deposition of metal-organic frameworks (MOF-CVD), is used for sensitizing silicon cantilevers. These cantilevers are coated with a uniform and compact Zn(EtIm)<sub>2</sub> (MAF-6) film, enabling the detection of volatile organic compounds (VOCs) through a change in the resonance frequency of the cantilever. The MOF-coated sensor exhibits remarkable sensitivity to VOCs within the 0.33 to 0.71 Hz/ppm range, and a limit of detection (LOD) spanning from 4 to 9 ppb. Notably, these sensitivities surpass those achieved by ZnO-coated cantilevers by two orders of magnitude. This high sensitivity is attributed to the high porosity and large surface area of MAF-6. The approach employed in this work is compatible with conventional microfabrication techniques and offers an advantageous avenue for the development of highly sensitive gas sensors.

**Keywords:** Metal-Organic Frameworks, thin films, VOCs, cantilever, gas sensor

## 1. Introduction

Volatile organic compounds (VOCs) are organic pollutants that are hazardous to the environment and human health. Monitoring and reducing VOC levels can improve indoor air quality and prevent negative health effects. Therefore, developing VOC sensors with high sensitivity, selectivity, low power consumption, and cost-effective manufacturing is crucial.

Metal-organic frameworks (MOFs) are a type of hybrid nanoporous crystalline materials. Zeolite imidazole frameworks (ZIFs) are MOFs where metals with tetrahedral coordination (i.e., Zn, Co, Fe, Cu) occupy the central node and the ligands are imidazolate-based organic molecules. ZIFs are promising for gas-sensing applications as they have a large surface area, high porosity, adjustable pore

size, and excellent selective adsorption capability for various gasses [1]. However, since ZIFs generally exhibit poor electrical conductivity, their application as the gas-sensing layer in conventional chemiresistive sensors is challenging. Therefore, these materials should be combined with conductive materials to form heterostructures and improve sensing performance [2][3]. These techniques can be complicated and challenging [4].

One possible approach to overcome this problem is using gravimetric transducers as a gas-sensing platform, such as microcantilevers, where the signal is generated based on the mass-change effect induced by gas adsorption. Microcantilevers are promising gravimetric transducers with high sensitivity and fast response [5]. The surface of the cantilever is generally coated with a sensing layer and the cantilever responds to analytes by either deflection (static mode) or a resonance frequency shift (dynamic mode).

Cantilevers have been sensitized by MOFs through direct solvothermal synthesis [6][7], or inkjet printing [8][9]. These techniques rely on solvothermal protocols and powder preparation routes which are not compatible with conventional microfabrication [10]. Recently, a new vapor-phase approach, called MOF-CVD, has been introduced, in which an oxide thin film is first deposited on a substrate via an established process, such as atomic layer deposition (ALD), and then the oxide is transformed into a MOF by exposing it to the vapor of an organic ligand. This technique is cleanroom compatible and enables the integration of MOF materials in microelectronic devices [11][12][13].

In this study, we employed the MOF-CVD technique to sensitize a silicon cantilever with a compact and uniform zinc 2-ethylimidazolate ( $\text{Zn}(\text{EtIm})_2$ ) thin film for VOC sensing. Unlike the organic linker in ZIF-8 (2-methylimidazolate), a commonly used gas-sensitive material, the organic linker in this MOF is less toxic, poses fewer safety concerns, and is easier to evaporate. To assess its performance, we conducted a comparative analysis with a cantilever sensitized with a ZnO thin film, considering the widespread use of ZnO as a gas sensing material [14]. Notably, our MOF-based device exhibited remarkable sensitivity to organic molecules (0.33 to 0.71 Hz/ppm range), with a detection limit in the range 4 to 9 ppb, surpassing the achieved with ZnO-coated cantilevers by two orders of magnitude.

## 2. Experimental Section

**Microcantilever sensors.** OCTOSENSIS dynamic-mode silicon cantilevers containing eight cantilevers per chip were purchased from Micromotive MIKROTECHNIK (Figure S1 (a)). The cantilever dimensions are  $L = 500 \pm 4 \mu\text{m}$ ,  $W = 90 \pm 2 \mu\text{m}$ , and  $H = 5 \pm 0.3 \mu\text{m}$ . The first three natural frequencies of the cantilevers operated in the bending mode are shown in Figure S1 (b).

**ZnO deposition.** ZnO was deposited using a homemade atmospheric-pressure spatial atomic layer deposition (AP-SALD) system equipped with a close-proximity gas injection head. Diethyl zinc (Aldrich) and deionized water were used as the metal and oxygen precursors, respectively, and nitrogen as the carrier gas. The precursor was bubbled and transported to the gas injector through a pure nitrogen flow (23 sccm). At the exit of the bubblers, another nitrogen flow (127 sccm), also called the dilution flow, was employed to regulate the concentration of the precursor in the gas phase. Similarly, the values used for carrying water vapor to the substrate surface were 45 sccm and 255 sccm for bubbling and the dilution, respectively. The nitrogen flow in each purging channel was kept at 150 sccm. The head was placed at 150  $\mu\text{m}$  from the substrate, which was oscillated underneath at a speed of 30  $\text{cm}\cdot\text{s}^{-1}$ . The substrate temperature was maintained at 200  $^{\circ}\text{C}$  during film deposition; more details about the AP-SALD technique are reported elsewhere [15][16].

**Synthesis of MOF.**  $\text{Zn}(\text{EtIm})_2$  was synthesized through the MOF-CVD approach. The ZnO-coated substrates and cantilevers were positioned in a Pyrex bottle as the reaction system (Figure 1). 0.034 g of 2-ethylimidazole powder (98%, Thermo Scientific Chemicals) as the organic linker was placed at the bottom of the bottle. A small vessel containing 10 ml of water as the template was placed inside the bottle, separated from the linker. The reaction system was closed and placed inside an oven at 140  $^{\circ}\text{C}$  for 90 min to convert ZnO to MOF. Characterizations and gas sensing measurements were conducted on as-prepared samples without activation.

**Characterization.** Grazing incident x-ray diffraction (GI-XRD) patterns were obtained using a PANalytical X'pert Pro MRD diffractometer with a  $\text{Cu K}\alpha$  source (1.54  $\text{\AA}$ ) at an incident angle of  $\omega=1^{\circ}$ . Surface morphologies were studied by field-emission scanning electron microscopy (FE-SEM, JOEL JSM 7200-F) and atomic force microscopy (AFM, Bruker Dimension FastScan).

**Experimental setup.** The chip was clamped to a piezoelectric actuator (Bruker DCHNM probe holder) and the device was excited by AC voltage. The vibration of the cantilever was measured by optical vibrometry (Polytec OFV 3001), whereby a laser beam was focused on the cantilever tip through a microscope with a 20x objective lens. The drive voltage and detection signals were supplied and controlled by a lock-in amplifier (Zurich Instruments HF2LI). The phase between the input and output signals was locked at the resonance of the second out-of-plane flexural mode and its frequency shift was monitored in real-time through the Phase-Locked Loop (PLL) built-in circuitry of the HF2LI. The chip was placed in a custom-made test chamber equipped with an optical window, a gas inlet and a gas outlet. Gas vapors were generated by passing a carrier gas (nitrogen) through a bubbler containing a liquid sample. The passage of nitrogen helped to evaporate the liquid. The total flow entering the test chamber was maintained at a constant value of 200 sccm throughout the experiment. The bubbler and

dilution flow rates were controlled by mass flow controllers (MFCs). The methodology for determining analyte concentration is detailed in the supplementary information. Figure S2 shows a schematic representation of the experimental setup.

### 3. Results and discussion

The GI-XRD pattern of the MOF grown from a 30 nm thick ZnO coating on a silicon substrate is shown in Figure 2. The peaks observed between 5° to 20° match the simulated pattern of Zn(EtIm)<sub>2</sub> with RHO topology (CSD Ref. Code: MECWOH). This MOF, known as MAF-6 in literature, is composed of tetrahedrally coordinated zinc cation centers, bridged by 2-ethylimidazole linker [17][18]. The main peaks between 30° to 40° correspond to the diffraction planes (100), (002), and (101) of ZnO, indicating the presence of residual ZnO underneath the MOF due to incomplete conversion. The presence of residual ZnO is commonly observed when its thickness exceeds a certain threshold [13]. However, it is important to note that gas sensing primarily occurs at the surface, which in this case is the MOF.

Achieving effective sensitization of microcantilevers with MOF requires optimizing the reaction conditions in advance. The sensitivity of microcantilever sensors is inversely proportional to their effective mass [19], and adding ZnO to the microcantilevers, followed by its conversion to MOF, increases their overall mass. Therefore, it is necessary to keep the thickness of the ZnO sacrificial layer at a minimum to prevent excessive mass addition to the sensors. On the other hand, an insufficient ZnO layer can cause non-uniform MOF film growth due to faster ZnO depletion and earlier crystallite ripening [13]. To identify the thinnest ZnO layer that could lead to uniform MOF formation, different thicknesses of ZnO were deposited on silicon substrates and converted to MOF. Figure 3 presents the surface morphology of ZnO sacrificial layers ranging from 10 to 30 nm and their corresponding MOF structures. The polycrystalline ZnO film has a grain morphology that evolves with thickness, where the thicker film has larger ZnO crystals. The deposition of 10 nm of ZnO leads to scattered MOF crystals on the substrate, while thicker oxide films provide more Zn species for the chemical reaction, causing the crystals to combine and form a uniform and compact MOF film. The results indicate that a 30 nm ZnO layer is suitable for cantilever functionalization. Nevertheless, based on the GI-XRD pattern (Figure 2), residual ZnO may be present beneath the MOF, which may influence the mechanical properties of the cantilever, such as its Young's modulus and structural damping. Consequently, this may affect the cantilever's natural frequency and quality factor, warranting further optimization of reaction temperature and duration. I. Stassen *et al.*[11] were able to achieve a continuous MOF without any residual ZnO by transforming a ZnO film with a thickness of less than 10 nm. However, it is important to consider that the organic linker used in their study, as well as their temperature and reaction duration, may not be identical to the conditions employed in this particular work. According to AFM

images, the ZnO and MOF surface roughness is 5.6 nm and 60 nm, respectively (Figure 4). Cross-sectional SEM images show that the thickness of the MOF on silicon is approximately 0.5  $\mu\text{m}$  (Figure S3).

Figure 5 shows a silicon cantilever (Figure 5 (a)) coated with 30 nm of ZnO (Figure 5 (b)) and subsequently converted to MOF (Figure 5 (c)). AP-SALD exposes all surfaces of the cantilevers to precursors, resulting in a conformal growth of ZnO, i.e. on all sides of the beam. Likewise, due to the gas-phase nature of the MOF-CVD process, all surfaces of the cantilever will be coated with MOF. This provides more surface area for gas adsorption. Furthermore, the conversion of ZnO to MOF results in a substantial thickness increase (as shown in Figure S3), which might induce surface tension and lead to the bending of the cantilever, if coated only on one side of it. Growing MOF uniformly on all sides of the cantilever can compensate for the surface tension and prevent the beam from bending. While this approach may alter the stiffness and mass of the cantilever, our measurements show that the frequency shifts between the silicon and the MOF-coated cantilevers were minimal, less than 1 kHz. This indicates that eventual changes in stiffness are also minimal.

The ZnO-coated and MOF-coated microcantilevers described above were deployed as gas sensors. In order to achieve higher mass sensitivity, the sensors were set to exploit the frequency shift of the second bending mode [20][21]. We identified the resonant frequency of that mode by sweeping the excitation frequency up in the vicinity of the natural frequency measured above while holding the amplitude constant at 0.5 V. The amplitude and phase of the measured voltage are depicted in Figure S4. They show that the resonant frequencies in air were  $f_o = 164.89$  kHz for the ZnO sensor and  $f_o = 164.06$  kHz for the MOF sensor.

The PLL of the lock-in amplifier was used to lock the sensor response at the resonant phase corresponding to  $f_o$ . The lock-in amplifier was then used to measure the frequency shift of that phase angle for both sensors as they were exposed to various environments. Figure 6 displays the real-time frequency shift when exposed to acetone, ethanol, isopropanol, and humidity. The shift is measured with respect to a baseline (reference) resonant frequency measured after the test chamber was purged with nitrogen and the sensor allowed to come to equilibrium with the nitrogen environment. Upon introducing each of the gas analytes into the chamber, the resonant frequency decreased monotonically with time until it reached equilibrium. The measurements were conducted across multiple cantilevers to validate the observed trend and ensure reproducibility.

The frequency shifts directly correlate with analyte concentration, wherein higher concentrations yield larger shifts. After purging the test chamber with nitrogen, the frequency shift reverts to zero. The MOF

sensors demonstrated larger frequency shifts and higher sensitivity to lower analyte concentrations than the ZnO sensors. Notably, the ZnO sensors exhibited minimal sensitivity to humidity.

The oscillator's frequency, governed by  $f = \sqrt{k/m}$ , can decrease due to changes in stiffness or mass. The observed drop in frequency is due to increased mass as the analyte adsorbs on the cantilever. It may also be a result of a drop in stiffness due to changes in material properties in the presence of the analyte [19]. The response time ( $t_{res}$ ) and the recovery time ( $t_{rec}$ ), measured as the time to reach 90% of final and initial values, respectively, (Figure S5) [22][23] are listed in Table 1 for each analyte. The measured response and recovery times combined with the consistency of the baseline across multiple sensing cycles, indicate that physisorption is the predominant process based on van der Waals interaction and is completely reversible, while chemisorption has no or minimal effect. The increased length of  $t_{res}$  for the MOF sensor can be attributed to the presence of a larger number of available adsorption sites for analytes on the MOF surface. As a result, it takes a longer time for the analyte to saturate the surface. However, it is important to note that both  $t_{res}$  and  $t_{rec}$  values are estimates and can be influenced by experimental procedures and conditions.

The sensors' responsivities were determined by plotting the frequency shift versus analyte concentration (Figure 7). The MOF sensors displayed high sensitivity to VOCs (with responsivities in the range of 0.33-0.71 Hz/ppm), exhibiting no clear selectivity among the VOCs but low sensitivity to humidity (0.02 Hz/ppm). Comparing these values with those for the ZnO sensors (Figure 7(a) and Table 1) highlights a remarkable improvement in sensitivity (by 80 to 250 times) due to the transformation of ZnO to MAF-6.

MAF-6 is a highly porous material with a large surface area, providing numerous adsorption sites. Previous studies have reported that the aperture size and pore size of MAF-6 is 7.1-7.6 Å and 18.1-18.8 Å, respectively, as determined through experiments and simulation [13][24]. These dimensions are larger than the molecular sizes of the analytes under test, indicating that MAF-6 can effectively accommodate a wide range of analytes of various sizes, resulting in superior sensitivity compared to ZnO. Several factors influence sensitivity, including the polarity of bonds, size of analyte molecules, and density of available active sites [25]. Since mass change is an important factor in inertial sensing, it is expected that isopropanol had the highest responsivity since its molecules are heavier than the other analytes. Similarly, acetone, which has a higher molar mass than ethanol, exhibits higher responsivity in the ZnO sensors. On the other hand, the responsivity of the MOF sensors to ethanol was slightly higher than that to acetone. This may be attributed to the smaller size of ethanol molecules facilitating their diffusion into the pores of the MOF or changes in the stiffness of the sensor material. These results show that in addition to showing a higher responsivity and lower LOD, MOF cantilever sensors may

offer additional approaches towards selectivity through the different diffusion and interaction mechanisms of different analytes with the MOF, and thus deserve further studies.

The calculated responsivity of both the ZnO- and MOF-coated cantilevers to humidity is significantly lower than that observed for the other analytes. While a lower sensitivity to humidity is expected due to water's lower molecular mass, the observed values are much lower than anticipated.

The limit of detection (LOD), the lowest concentration of an analyte that can be accurately detected, is a function of the sensor responsivity (R) and background noise ( $LOD = 3 \frac{\Delta f_{noise}}{R}$ ) [26]. Given a measured noise floor of  $\Delta f_{noise} = 0.001$  Hz (Figure S6), the LODs of the sensors were calculated as listed in Table 1. The LOD of MOF sensors for VOCs is in the parts per billion (ppb) range, which is three orders of magnitude better than that of the ZnO sensor. A comparison of inertial sensors in which MOFs are utilized as the sensing material is presented in Table 2. The MOF sensors demonstrated in this work have the lowest LOD. However, the performance of a cantilever-based sensor is influenced by multiple factors beyond just the sensing material, such as cantilever dimensions, sensor actuation, read-out scheme, and system noise. A precise comparison between MAF-6 and other MOFs would require conducting experiments under identical conditions, providing a promising avenue for future investigations.

#### **4. Conclusions**

In conclusion, the MOF-CVD approach was utilized to sensitize silicon cantilevers with a MOF as a sensing layer for the detection of VOCs, and the sensing performance was compared with cantilevers sensitized with a ZnO thin film. The MOF-coated sensor exhibited superior sensitivity to VOCs, with LODs in the range of ppb, thanks to the high porosity and large surface area of MAF-6. We hypothesize that the initial resonance frequency measurements conducted under vacuum conditions may have facilitated the activation of the MOF by removing excess molecules from the pores. Thermal activation of MAF-6 could yield even more promising gas-sensing results, remaining for future exploration. The sensitivities can be further improved by reducing the dimensions of the microcantilever and enhancing the actuation and read-out scheme. This technique is solvent-free and compatible with conventional microfabrication processes, making it a promising candidate for the fabrication of highly sensitive gas sensors.

#### **Supplementary Material**

See the supplementary materials for additional information, including experimental setup details, cross-section SEM images, natural frequency measurements, analyte concentration calculations, and system noise and LOD estimations.

### Acknowledgments

M.A acknowledges a Mitacs Globalink Research Award. K. M. acknowledges support from the Waterloo Institute for Nanotechnology and National Research Council of Canada Joint Seed Funding program, Canada Foundation for Innovation John R. Evans Leaders Fund (Project 35552), and Ontario Research Fund - Research Infrastructure (Project 35552). D.M.-R. and C.C. acknowledge support from the FETOPEN-1-2016-2017 research and innovation program under Grant Agreement 801464 (SPRINT).

### References

- [1] T. Shi, S. Hussain, C. Ge, G. Liu, M. Wang, and G. Qiao, "ZIF-X (8, 67) based nanostructures for gas-sensing applications," *Rev. Chem. Eng.*, vol. 39, no. 6, pp. 911–939, 2023.
- [2] X. F. Wang, X. Z. Song, K. M. Sun, L. Cheng, and W. Ma, "MOFs-derived porous nanomaterials for gas sensing," *Polyhedron*, vol. 152, pp. 155–163, 2018.
- [3] H. Yuan, N. Li, W. Fan, H. Cai, and D. Zhao, "Metal-Organic Framework Based Gas Sensors," *Adv. Sci.*, vol. 9, no. 6, p. 2104374, 2022.
- [4] P. Kumar, K. H. Kim, P. K. Mehta, L. Ge, and G. Lisak, "Progress and challenges in electrochemical sensing of volatile organic compounds using metal-organic frameworks," *Crit. Rev. Environ. Sci. Technol.*, vol. 49, no. 21, pp. 2016–2048, 2019.
- [5] K. M. Goeders, J. S. Colton, and L. A. Bottomley, "Microcantilevers: Sensing chemical interactions via mechanical motion," *Chem. Rev.*, vol. 108, no. 2, pp. 522–542, 2008.
- [6] C. Yim *et al.*, "Adsorption and desorption characteristics of alcohol vapors on a nanoporous ZIF-8 film investigated using silicon microcantilevers," *Chem. Commun.*, vol. 51, no. 28, pp. 6168–6171, 2015.
- [7] S. Cai *et al.*, "In situ construction of metal-organic framework (MOF) UiO-66 film on Parylene-patterned resonant microcantilever for trace organophosphorus molecules detection," *Analyst*, vol. 144, no. 12, pp. 3729–3735, 2019.

- [8] Y. Lv, H. Yu, P. Xu, J. Xu, and X. Li, "Metal organic framework of MOF-5 with hierarchical nanopores as micro-gravimetric sensing material for aniline detection," *Sensors Actuators B*, vol. 256, pp. 639–647, 2018.
- [9] P. Xu, T. Xu, H. Yu, and X. Li, "Resonant-Gravimetric Identification of Competitive Adsorption of Environmental Molecules," *Anal. Chem.*, vol. 89, no. 13, pp. 7031–7037, 2017.
- [10] I. Stassen, N. Burtch, A. Talin, P. Falcaro, M. Allendorf, and R. Ameloot, "An updated roadmap for the integration of metal–organic frameworks with electronic devices and chemical sensors," *Chem. Soc. Rev.*, vol. 46, no. 11, pp. 3185–3241, 2017.
- [11] I. Stassen *et al.*, "Chemical vapour deposition of zeolitic imidazolate framework thin films," *Nat. Mater.*, vol. 15, no. 3, pp. 304–310, 2016.
- [12] A. J. Cruz *et al.*, "Integrated cleanroom process for the vapor-phase deposition of large-area zeolitic imidazolate framework thin films," *Chem. Mater.*, vol. 31, no. 22, pp. 9462–9471, 2019.
- [13] T. Stassin *et al.*, "Solvent-Free Powder Synthesis and MOF-CVD Thin Films of the Large-Pore Metal-Organic Framework MAF-6," *Chem. Mater.*, vol. 32, no. 5, pp. 1784–1793, Mar. 2020.
- [14] Y. Kang, F. Yu, L. Zhang, W. Wang, L. Chen, and Y. Li, "Review of ZnO-based nanomaterials in gas sensors," *Solid State Ionics*, vol. 360, no. December 2020, p. 115544, 2021.
- [15] V. H. Nguyen *et al.*, "Deposition of ZnO based thin films by atmospheric pressure spatial atomic layer deposition for application in solar cells," *J. Renew. Sustain. Energy*, vol. 9, no. 2, p. 21203, 2017.
- [16] R. L. Z. Hoye, D. Muñoz-Rojas, K. P. Musselman, Y. Vaynzof, and J. L. MacManus-Driscoll, "Synthesis and Modeling of Uniform Complex Metal Oxides by Close-Proximity Atmospheric Pressure Chemical Vapor Deposition," *ACS Appl. Mater. Interfaces*, vol. 7, no. 20, pp. 10684–10694, 2015.
- [17] Z. Akimbekov *et al.*, "Experimental and Theoretical Evaluation of the Stability of True MOF Polymorphs Explains Their Mechanochemical Interconversions," *J. Am. Chem. Soc.*, vol. 139, no. 23, pp. 7952–7957, 2017.
- [18] B. Mortada, G. Chaplais, H. Nouali, C. Marichal, and J. Patarin, "Phase Transformations of Metal-Organic Frameworks MAF-6 and ZIF-71 during Intrusion-Extrusion Experiments," *J.*

- Phys. Chem. C*, vol. 123, no. 7, pp. 4319–4328, 2019.
- [19] B. N. Johnson and R. Mutharasan, “Biosensing using dynamic-mode cantilever sensors: A review,” *Biosens. Bioelectron.*, vol. 32, no. 1, pp. 1–18, 2012.
- [20] S. Dohn, R. Sandberg, W. Svendsen, and A. Boisen, “Enhanced functionality of cantilever based mass sensors using higher modes,” *Appl. Phys. Lett.*, vol. 86, no. 23, pp. 1–3, Jun. 2005.
- [21] M. Narducci *et al.*, “Sensitivity improvement of a microcantilever based mass sensor,” *Microelectron. Eng.*, vol. 86, no. 4–6, pp. 1187–1189, 2009.
- [22] J. Dai *et al.*, “Printed gas sensors,” *Chem. Soc. Rev.*, vol. 49, no. 6, pp. 1756–1789, 2020.
- [23] G. W. Hunter *et al.*, “Editors’ Choice—Critical Review—A Critical Review of Solid State Gas Sensors,” *J. Electrochem. Soc.*, vol. 167, no. 3, p. 037570, 2020.
- [24] C. T. He *et al.*, “Exceptional Hydrophobicity of a Large-Pore Metal-Organic Zeolite,” *J. Am. Chem. Soc.*, vol. 137, no. 22, pp. 7217–7223, Jun. 2015.
- [25] F. Ullah *et al.*, “WS 2 and WS 2 -ZnO Chemiresistive Gas Sensors: The Role of Analyte Charge Asymmetry and Molecular Size ,” *ACS Sensors*, 2023.
- [26] C. K. McGinn, Z. A. Lamport, and I. Kyriassis, “Review of Gravimetric Sensing of Volatile Organic Compounds,” *ACS Sensors*, vol. 5, no. 6, pp. 1514–1534, 2020.
- [27] H. H. Yeung, G. Yoshikawa, K. Minami, and K. Shiba, “Strain-based chemical sensing using metal-organic framework nanoparticles,” *J. Mater. Chem. A*, vol. 8, no. 35, pp. 18007–18014, 2020.
- [28] T. Xu, P. Xu, D. Zheng, H. Yu, and X. Li, “Metal-organic frameworks for resonant-gravimetric detection of trace-level xylene molecules,” *Anal. Chem.*, vol. 88, no. 24, pp. 12234–12240, 2016.
- [29] J. Devkota, K. J. Kim, P. R. Ohodnicki, J. T. Culp, D. W. Greve, and J. W. Lekse, “Zeolitic imidazolate framework-coated acoustic sensors for room temperature detection of carbon dioxide and methane,” *Nanoscale*, vol. 10, no. 17, pp. 8075–8087, 2018.
- [30] Y. Hwang, A. Phan, K. Galatsis, O. M. Yaghi, and R. N. Candler, “Zeolitic imidazolate framework-coupled resonators for enhanced gas detection,” *J. Micromechanics Microengineering*, vol. 23, no. 12, 2013.

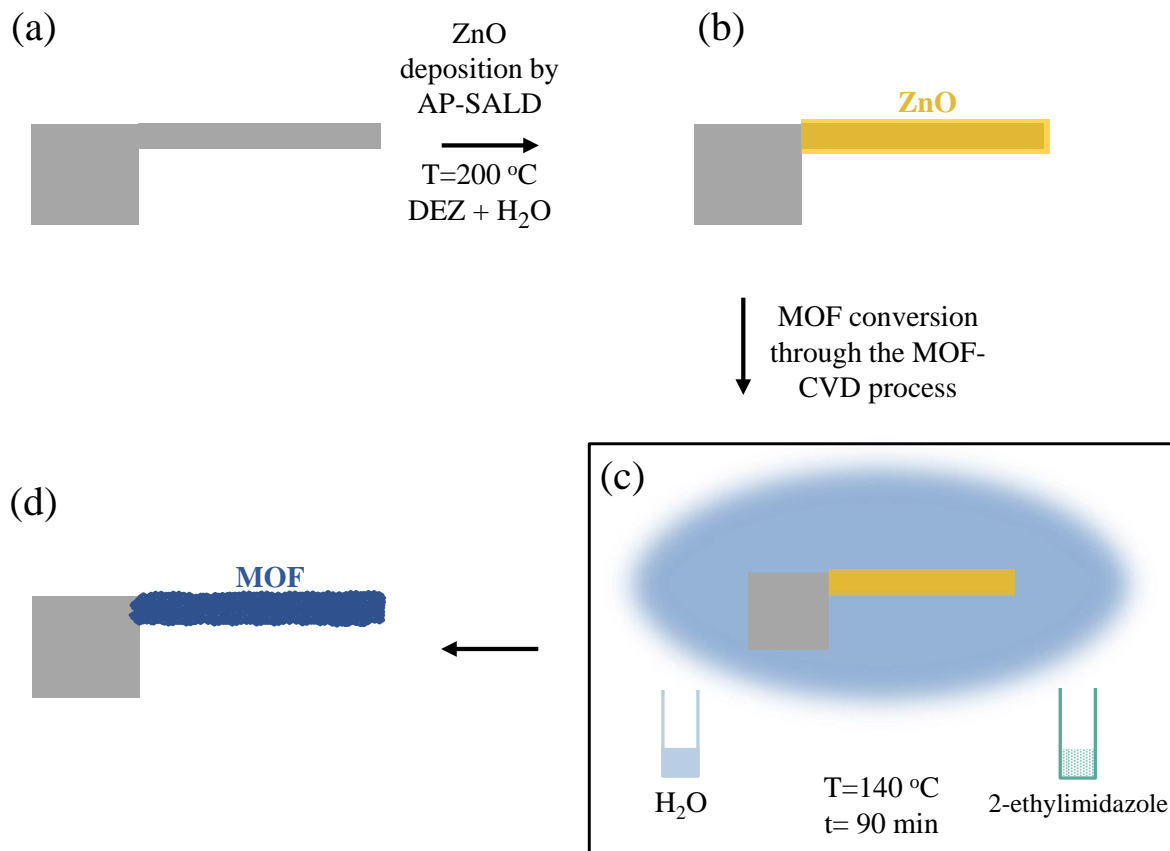


Figure 1. Schematic representation of sensitization of cantilevers with  $\text{Zn}(\text{EtIm})_2$  through MOF-CVD process. A silicon cantilever (a) is coated with 30 nm of ZnO by atmospheric-pressure spatial atomic layer deposition (AP-SALD) (b). Then the cantilever is placed in a bottle with 2-ethylimidazole and  $\text{H}_2\text{O}$  (c). The reaction takes place at 140 °C for 90 min, and ZnO converts to MOF on the surface of the cantilever (d).

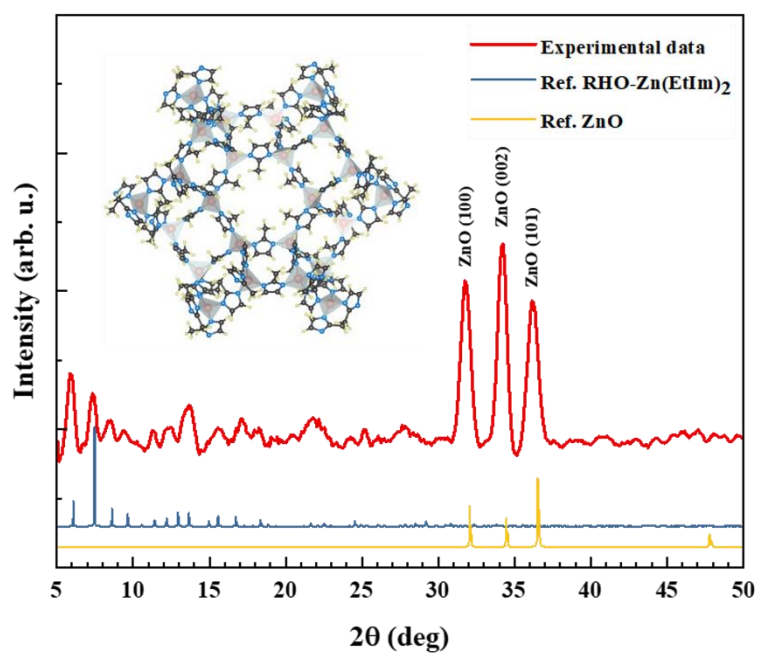


Figure 2. GI-XRD pattern obtained from the MOF (red) which was transformed from 30 nm of ZnO on a silicon substrate. Reference patterns of ZnO (yellow, COD number: 96-900-4180), and RHO-Zn(EtIm)<sub>2</sub> (blue, CSD Ref. Code: MECWOH). The inset depicts the crystal structure of RHO-Zn(EtIm)<sub>2</sub>.

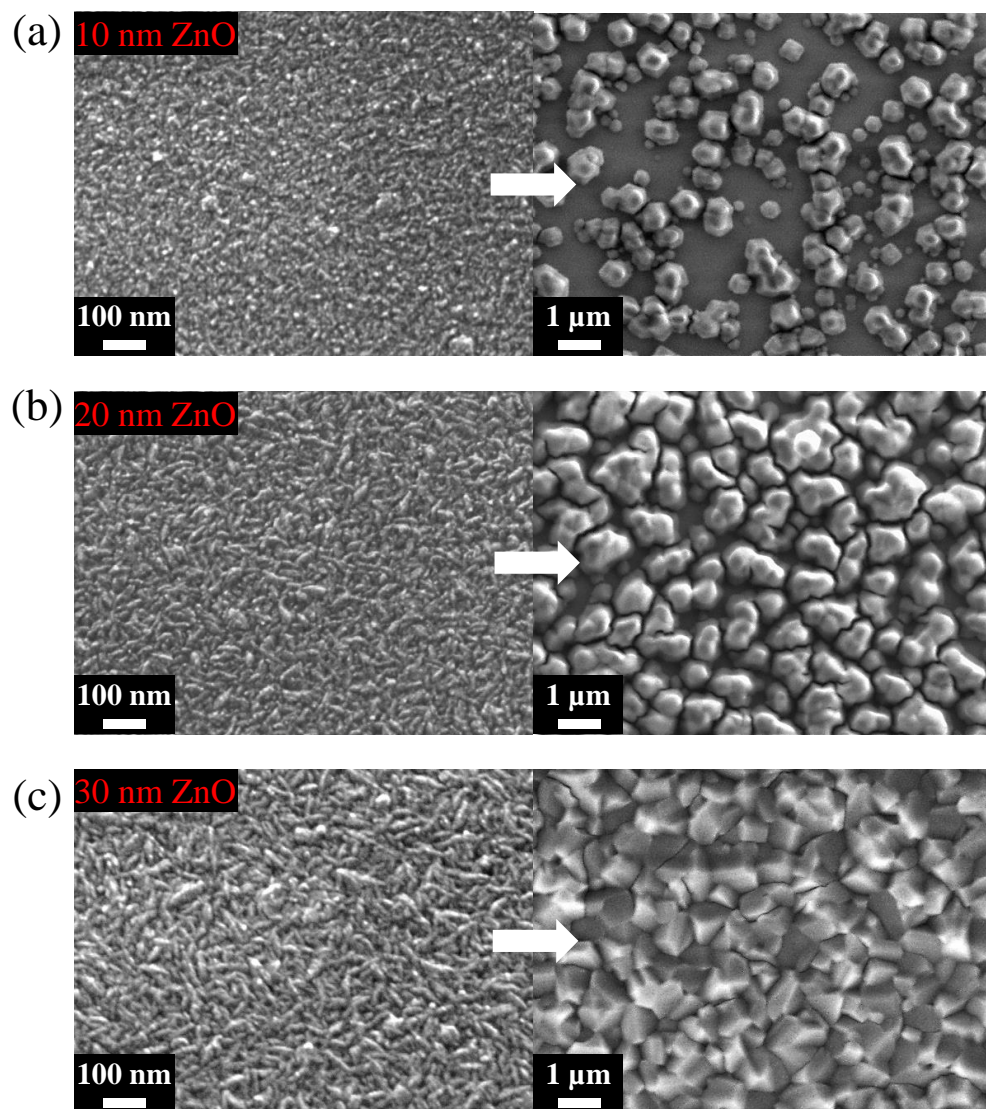


Figure 3. SEM images of (a) 10 nm, (b) 20 nm, and (c) 30 nm of ZnO (left) transformed to MOF (right). The reaction duration and temperature are 90 min and 140 °C, respectively.

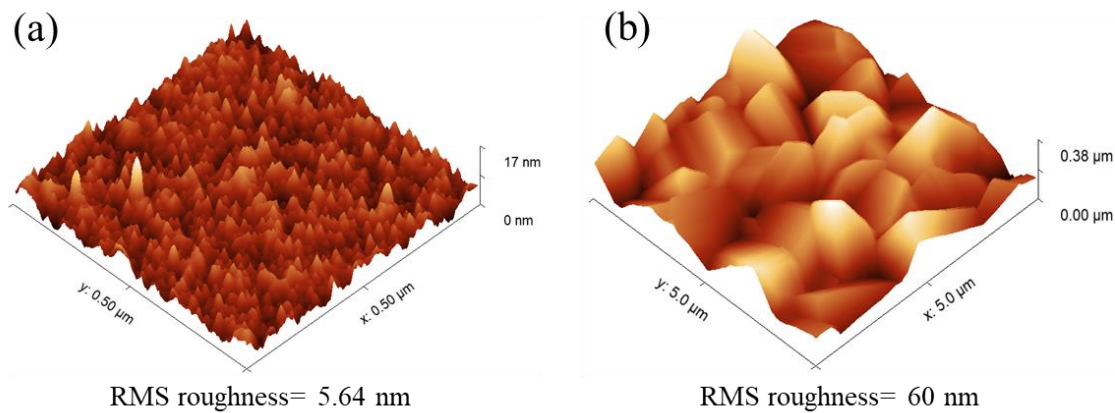


Figure 4. AFM images of (a) 30 nm ZnO (b) transformed to MOF.

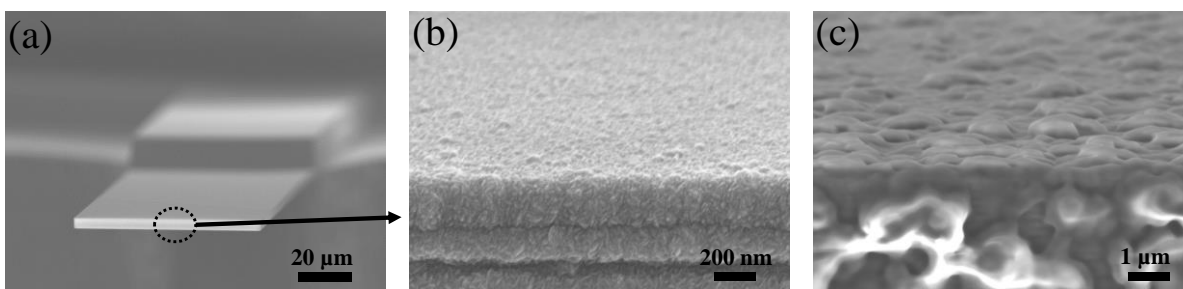


Figure 5. SEM images of (a) an uncoated silicon microcantilever, and the edge of the microcantilever (b) coated with 30 nm of ZnO and (c) transformed to MOF.

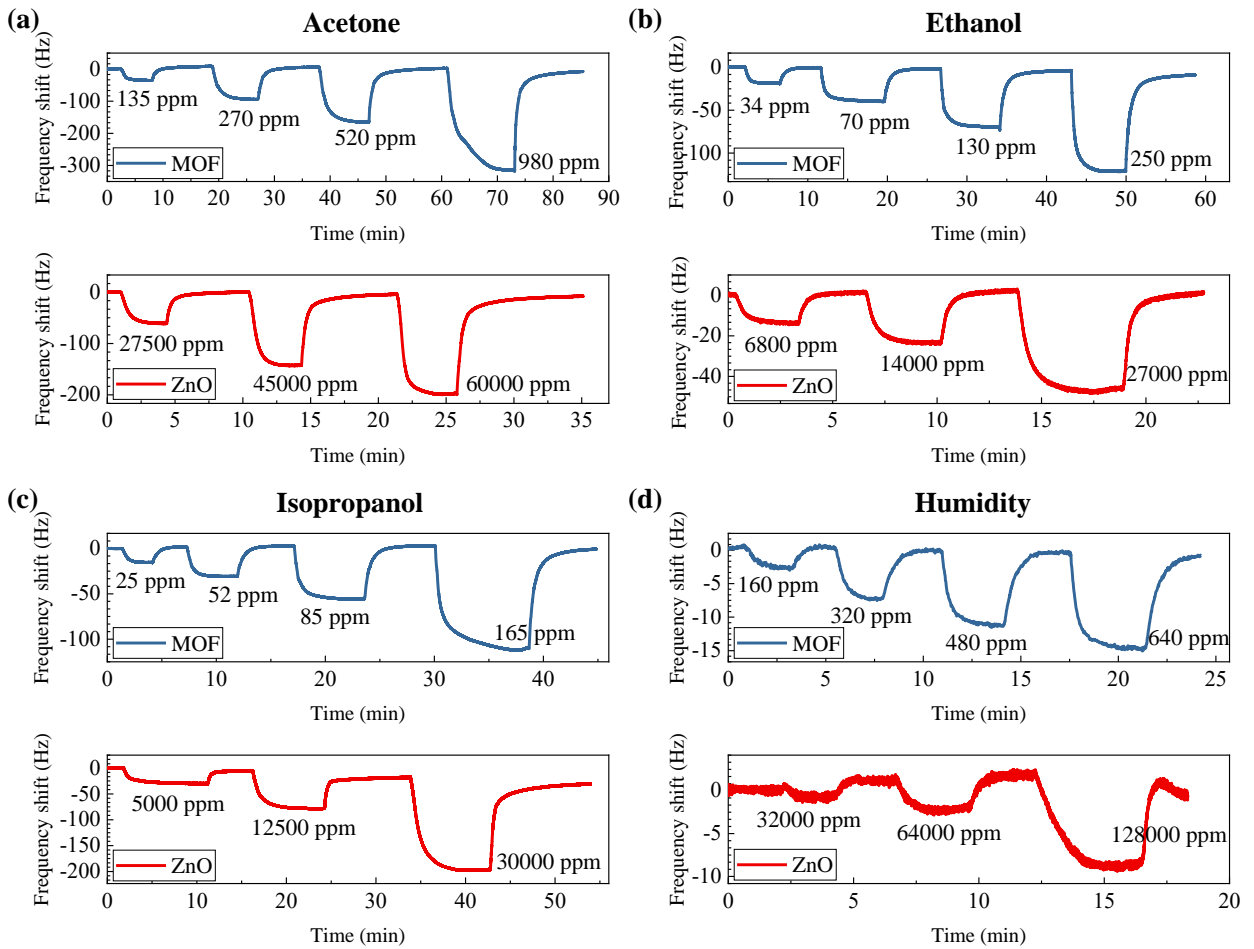


Figure 6. Frequency shift over time of the ZnO and MOF sensors in response to the injection of different ppm of (a) acetone, (b) ethanol, (c) isopropanol, and (d) humidity followed by respective purges.

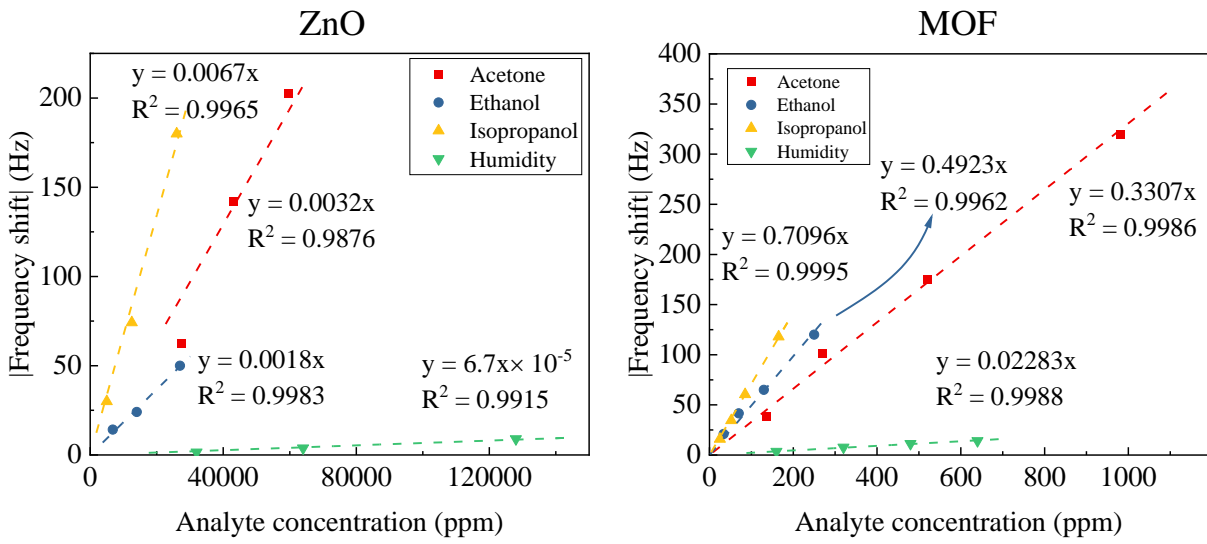


Figure 7. The frequency shifts of the (a) ZnO and (b) MOF sensors versus analyte concentrations.

Table 1. Summary of gas sensing results for the MOF-coated and ZnO-coated sensors.

Analyte (Size, molar mass)	MOF			ZnO		
	Responsivity (Hz/ppm)	Response/Recovery time (s)	Limit of detection (ppm)	Responsivity (Hz/ppm)	Response/Recovery time (s)	Limit of detection (ppm)
Acetone (4.6 Å, 58.08 g/mol)	0.33	175 / 185	0.0091	$3.2 \times 10^{-3}$	85 / 90	1.3
Ethanol (4.5 Å, 46.07 g/mol)	0.49	120 / 125	0.0051	$1.8 \times 10^{-3}$	85 / 55	1.6
Isopropanol (4.7 Å, 60.1 g/mol)	0.71	66 / 76	0.0042	$6.7 \times 10^{-3}$	140 / 120	0.5
Humidity (2.75 Å, 18.01 g/mol)	0.02	69 / 88	0.15	$6.7 \times 10^{-5}$	—	—

Table 2. Comparison of gravimetric sensors in which MOFs are utilized as the sensing material.

Ref.	MOF	Fabrication method	Device type	Analyte	Responsivity	$t_{res}$	LOD
						$t_{rec}$	
This work	MAF-6	MOF-CVD	Cantilever (dynamic)	Acetone, ethanol, isopropanol	0.33 – 0.71 Hz/ppm	120 – 180 s	4 – 9 ppb
						120 – 180 s	
[6]	ZIF-8	Solvothermal	Cantilever (static and dynamic)	Methanol, ethanol, 1-propanol	-	10 – 100 s	N/A
						>1000 s	
[27]	ZIF-7, 8, 65, 71	Inkjet printing	Membrane-type surface stress Sensor (MSS)	Various VOCs	N/A	1 – 30 s	0.1-30 ppm
						10 – 30 s	
[8]	MOF-5	Inkjet printing	Cantilever (dynamic)	Aniline	0.1 – 0.5 Hz/ppm	108 s	1.4 ppm
[28]	HKUST	Micro-plotting	Cantilever (dynamic)	Xylene	0.1 – 2.3 Hz/ppm	200 – 400 s	400 ppb
						400 – >1500 s	
[29]	ZIF-8	Solution processing	QCM; SAW	CO <sub>2</sub> , CH <sub>4</sub>	0.01-1.44 × 10 <sup>-6</sup> /vol%	N/A	N/A
[30]	ZIF-69	Drop casting	Double-clamped resonator	CO <sub>2</sub> , 2-propanol	0.15 – 3.5	10 – 100 s	15 ppm